2016 IEEE 55th Conference on Decision and Control (CDC)
ARIA Resort & Casino
December 12-14, 2016, Las Vegas, USA

Joint Order Identification and Estimation of the Discrete Relaxation Spectrum for Ground Penetrating Radars

Ahmad A. Masoud, Ali Al-Shaikhi

Abstract— **This paper suggests a novel procedure to jointly identify the order of a GPR discrete relaxation spectrum and estimate its parameters (relaxation frequencies and their strengths). These quantities are important for interpreting the contents of the subsurface layers. The suggested method turns the estimator into a nonlinear control system that can convert an initial guess of the number and parameters of the relaxation modes into the correct one. Blindly identifying the number of relaxation modes and estimating their values and strengths is guaranteed if the number of assumed modes is higher than the number of actual modes. The procedure is hardware-friendly and exhibit high resistance to noise.**

I. INTRODUCTION

Ground penetrating radars are electromagnetic-based techniques used to provide visual indicators of the contents of shallow subsurface areas. They have many applications in construction, nondestructive testing and landmine detection to mention a few [1,2]. GPRs operate by radiating a spectrum-rich signal into the ground that is to be explored. The radiated signal travels through the earth's sub-layers. The objects that the traveling wave encounters either reflect or absorb part of the wave energy. Some of the absorbed component causes the electromagnetic energy to resonate within these objects. The resonant energy that is trapped inside the objects quickly dissipates as part of it is re-radiated to the outside world. The reflected signal picked-up by a GPR's receiver at a location, known as the wiggle trace, is the building block of all GPR subsurface images. A wiggle trace may be used at a location to detect the presence of objects and to determine how deep they lie beneath the surface.

Subsurface materials are often described as dielectrics, with the parameters permittivity and conductivity loosely termed as their 'dielectric properties' [3]. As electromagnetic energy moves through a medium, charges become displaced and polarized, resulting in a loss of energy [4, 5]. The frequency at which this polarization occurs is called the relaxation frequency. The resulting electrical losses are a major factor in determining how deep the incident wave can travel through earth. Moreover, these losses constitute a major part of the mechanism through which subsurface information is encoded in the reflected GPR signal. In effect, a GPR attempts to record the contrast of the earth's sub-layer dielectric properties. The dispersion and absorption of many liquids and dielectrics are represented [6] by the empirical formula:

$$\frac{c}{1+i\cdot\frac{\omega}{\zeta}} \tag{1}$$

where ζ is the generalized relaxation frequency and c is a constant representing the strength of this spectrum component. Using the above formula, the complex relaxation spectrum of a GPR trace may be modeled as:

$$H(\omega) = c_0 + \sum_{k=1}^{N} \frac{c_k}{1+i\cdot\frac{\omega}{\zeta_k}} \tag{2}$$

where N is the number of relaxation frequencies, c_k's and ζ_k's are their strengths and values. All these parameters are unknown and have to be estimated in order to form an idea about the subsurface content at the location where the reflected signal is acquired. This excessively complex task requires that model order identification and spectrum estimation [7, 8, 9] be jointly and accurately carried-out. What makes the process difficult is that the parametric spectrum of a reflected GPR signal does not conform to an ARMA model. This prevents the use of well-developed parametric spectrum estimation techniques.

A variety of procedures was suggested to identify the relaxation spectrum. An approach that uses the first and second derivative of the spectrum to compute the number and values of the relaxation frequencies is suggested in [10, 11]. The strengths of the relaxation modes are not estimated. Differentiating the spectrum of a real-life signal can make the estimates highly susceptible to noise. In another approach [12, 13] heuristics are used to determine the number and values of the relaxation frequencies. Linear regression is then used to compute the magnitudes of these frequencies. In [14, 15] a large number of relaxation frequencies along with their strengths is assumed. A computationally intensive nonlinear regression is applied to iteratively reduce the number of frequencies until the minimum components are reached that produce a satisfactory fit. An approach that capitulate on existing parametric spectrum estimation techniques starts by selecting a large number of possible relaxation frequency samples. The magnitudes of these frequencies are estimated.

*Resrach supported by King Fahad University of Petroleum & Minerals
Ahmad A. Masoud & Ali Al-Shaikhi are with the electrical engineering department, King Fahad University of Petroleum & Minerals, Dhahran, 31261, Saudi Arabia (e-mail:masoud@kfupm.edu.sa, shaikhi@kfupm.edu.sa)

Based on the magnitude estimates, procedures are developed to select the frequency samples that have high probability of belonging to the actual relaxation spectrum [16, 17, 18]. A considerable amount of work seems to focus on estimating the continuous distribution of the relaxation frequencies [19, 20]. However, [21] showed that the discrete relaxation spectrum carries almost all the information in the continuous spectrum. They prove that few relaxation modes can be used accurately to mimic the continuous spectrum.

This paper suggests a novel, joint order identification and discrete relaxation spectrum estimation procedure. The method can blindly and accurately compute the number of relaxation frequencies, their values and strengths. All what is required is that the initial number of frequency relaxation modes is equal to or higher than the actual number of frequency components that created the spectrum. Initially, the values and strengths of the relaxation frequencies can be selected arbitrarily. Informed selection can speed-up the convergence of the procedure. The method is relatively fast, hardware-friendly and has excellent performance in the presence of noise. The procedure is developed and its performance is thoroughly investigated by simulation.

II. PROBLEM STATEMENT

Let N be the true number of relaxation frequencies contained in the relaxation spectrum (equation-1). Let $\Psi = [\zeta_1 \quad \zeta_2 \quad .... \quad \zeta_N]^T$ be a vector containing the true relaxation frequencies and $C = [c_0 \quad c_1 \quad ... \quad c_N]^T$ be their corresponding strengths. Let Ns be the number of assumed relaxation modes. This number has to be greater than or equal to the actual number (Ns≥N). Let Ψs ($\Psi s = [\zeta s_1 \quad \zeta s_2 \quad .... \quad \zeta s_{Ns}]^T$) and Cs ($Cs = [cs_0 \quad cs_1 \quad ... \quad cs_{Ns}]^T$) be state variables used to estimate the relaxation frequencies and their strengths. Also, let H(Ω) be the discrete relaxation spectrum computed from a reflected wiggle trace and sampled at L discrete frequencies ($\Omega = [\omega_1 \quad \omega_2 \quad .. \quad \omega_L]$). The joint order identification and discrete relaxation spectrum estimation is carried-out by constructing the first order, nonlinear dynamical system in (3):

$$\begin{bmatrix} \dot{Cs} \\ \dot{\Psi s} \end{bmatrix} = F(Cs, \Psi s, H(\Omega)). \tag{3}$$

The system is constructed so that the final values of the state

$$\begin{bmatrix} Cf \\ \Psi f \end{bmatrix} = \lim_{t\to\infty} \begin{bmatrix} Cs(t) \\ \Psi s(t) \end{bmatrix} \tag{4}$$

satisfies $\forall \quad \zeta_i \in \Psi \quad i = 1,..N, \exists \zeta f_j \in \Psi f \quad \ni \zeta_i = \zeta f_j$ (5)

$$\forall \quad \zeta f_j \in \Psi f \quad j = 1,..Ns, \exists \zeta_i \in \Psi \quad \ni \zeta f_j = \zeta_i .$$

Also for $\zeta f_{I(k)} = \zeta_i, \quad k = 1,..M$

$$\sum_{k=1}^{M} cf_k = c_i \tag{6}$$

III. THE SPECTRUM ESTIMATOR

The suggested method begins by acquiring a reflected GPR trace. This trace is used to compute a sampled frequency spectrum vector H(Ω) (7). The method places little restrictions on the frequency points. One may densely sample the frequency spectrum in a uniform manner without suffering excessive computational complexity. On the other hand, extensive simulation shows that the method functions well even if the sample size is relatively small.

$$H(\Omega) = \begin{bmatrix} H(\omega_1) \\ . \\ H(\omega_L) \end{bmatrix} \tag{7}$$

The goal of the dynamical system in (3) is to drive the assumed discrete relaxation spectrum parameters to final values that satisfy the system in (8). The structure of the spectrum is factored in the evolution process to naturally filter-out erroneous estimate trajectories that yield incorrect values of the discrete relaxation parameters that may also satisfy equation (8).

$$\begin{bmatrix} H(\omega_1) \\ H(\omega_2) \\ . \\ H(\omega_L) \end{bmatrix} = \begin{bmatrix} 1 & \frac{1}{1+i\cdot\omega_1/\zeta f_1} & \cdots & \frac{1}{1+i\cdot\omega_1/\zeta f_{Ns}} \\ 1 & \frac{1}{1+i\cdot\omega_2/\zeta f_1} & \cdots & \frac{1}{1+i\cdot\omega_2/\zeta f_{Ns}} \\ \vdots & \vdots & : & \vdots \\ 1 & \frac{1}{1+i\cdot\omega_L/\zeta f_1} & \cdots & \frac{1}{1+i\cdot\omega_L/\zeta f_{Ns}} \end{bmatrix} \begin{bmatrix} cf_0 \\ cf_1 \\ \vdots \\ cf_{Ns} \end{bmatrix} \tag{8}$$

The construction of the system (3) begins by creating the expanded vector $H_e(\Omega)$ (9) that have the real and imaginary parts of H(Ω) explicitly stated

$$He(\Omega) = \begin{bmatrix} Re(H(\omega_1)) \\ . \\ Re(H(\omega_L)) \\ Im(H(\omega_1)) \\ . \\ Im(H(\omega_L)) \end{bmatrix} \tag{9}$$

A vector (Ha) is constructed representing the expanded transient, estimate spectrum (10) along with the reflection matrix T (11). Both are generated from the values of $\Psi s(t), Cs(t)$ at time t

$$Ha(\Omega, \Psi s, Cs) = \begin{bmatrix} cs_0 + \sum_{i=1}^{Ns} cs_i \cdot \frac{\zeta s_i}{(\zeta s_i)^2 + (\omega_1)^2} \\ . \\ cs_0 + \sum_{i=1}^{Ns} cs_i \cdot \frac{\zeta s_i}{(\zeta s_i)^2 + (\omega_L)^2} \\ -cs_0 - \sum_{i=1}^{Ns} cs_i \cdot \frac{\omega_1 \cdot \zeta s_i}{(\zeta s_i)^2 + (\omega_1)^2} \\ . \\ -cs_0 - \sum_{i=1}^{Ns} cs_i \cdot \frac{\omega_1 \cdot \zeta s_i}{(\zeta s_i)^2 + (\omega_L)^2} \end{bmatrix} \tag{10}$$

The order of the relaxation spectrum along with the values of the relaxation frequencies and their strengths may be obtained from the final value of the nonlinear state space system in (12)

$$T(\Omega,\Psi s,Cs)=\begin{bmatrix} \frac{1}{(\zeta s_1)^2+(\omega_1)^2} & \cdots & \frac{1}{(\zeta s_1)^2+(\omega_L)^2} & \cdots & \frac{0}{-\zeta s_1\cdot\omega_1} & \cdots & \frac{0}{-\zeta s_1\cdot\omega_L} \\ \frac{(\zeta s_{Ns})^2}{(\zeta s_{Ns})^2+(\omega_1)^2} & \cdots & \frac{(\zeta s_{Ns})^2}{(\zeta s_{Ns})^2+(\omega_L)^2} & \cdots & \frac{-\zeta s_{Ns}\cdot\omega_1}{(\zeta s_{Ns})^2+(\omega_1)^2} & \cdots & \frac{-\zeta s_{Ns}\cdot\omega_L}{(\zeta s_{Ns})^2+(\omega_N)^2} \\ 2\cdot cs_1\cdot\frac{\zeta s_1\cdot\omega_1^2}{[(\zeta s_1)^2+(\omega_1)^2]^2} & \cdots & 2\cdot cs_1\cdot\frac{\zeta s_1\cdot\omega_L^2}{[(\zeta s_1)^2+(\omega_L)^2]^2} & \cdots & cs_1\cdot\omega_1\cdot\frac{(\zeta s_1)^2-\omega_1^2}{[(\zeta s_1)^2+(\omega_1)^2]^2} & \cdots & cs_1\cdot\omega_L\cdot\frac{(\zeta s_1)^2-\omega_L^2}{[(\zeta s_1)^2+(\omega_L)^2]^2} \\ 2\cdot cs_{Ns}\cdot\frac{\zeta s_{Ns}\cdot\omega_1^2}{[(\zeta s_{Ns})^2+(\omega_1)^2]^2} & \cdots & 2\cdot cs_{Ns}\cdot\frac{\zeta s_{Ns}\cdot\omega_L^2}{[(\zeta s_{Ns})^2+(\omega_L)^2]^2} & \cdots & cs_{Ns}\cdot\omega_1\cdot\frac{(\zeta s_{Ns})^2-\omega_1^2}{[(\zeta s_{Ns})^2+(\omega_1)^2]^2} & \cdots & cs_{Ns}\cdot\omega_L\cdot\frac{(\zeta s_{Ns})^2-\omega_L^2}{[(\zeta s_{Ns})^2+(\omega_L)^2]^2} \end{bmatrix} \quad (11)$$

$$\begin{bmatrix}\dot{C}s\\ \dot{\Psi}s\end{bmatrix}=T(\Omega,\Psi s,Cs)\cdot(He(\Omega)-Ha(\Omega,\Psi s,Cs)) \quad (12)$$

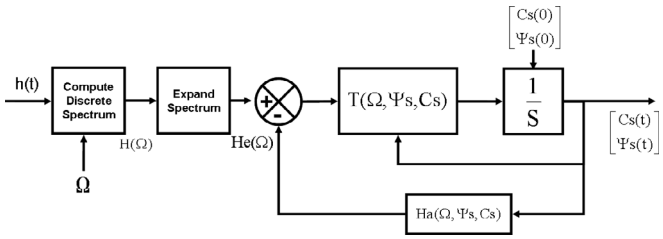

Figure-1: The suggested spectrum estimator

IV. SIMULATION RESULTS

This section contains simulation results to demonstrate the capabilities of the suggested method. The base truth used to test the estimator is obtained from equation (2).

1. Effect of false initial assumptions

This example demonstrates that the suggested method is able to eliminate superfluous assumptions of the spectrum components and produce both the number and parameters of the modes of the discrete relaxation spectrum. The base truth reflected signal is assumed to contain three relaxation frequencies. Their values and magnitudes are shown in table-1

ζ	0	10	50	900
C	1/2	1	1	3

Table-1: base-truth relaxation frequencies

The complex spectrum is evaluated at the 17 angular frequencies ω_i={30, 40, 50, 60, 70, 80, 90,100,200, 300, 400,500, 600, 700, 800, 900, 1000, 2000}.

Here the number of assumed relaxation frequencies is made the same as the base-truth ones. The initial guess (table-2) is:

ζs (0)	0	50.1	90.5	120
Cs (0)	0.7	3.8	4.2	2.8

Table-2: Initial guess

The final estimates are shown in table-3 and the evolution of the frequencies is shown in figure-2. As can be seen, all the assumed quantities converged close to the true ones.

ζf	0	12.1	45.6	890
Cf	0.521	.79	1.09	3.03

Table-3: Final estimates

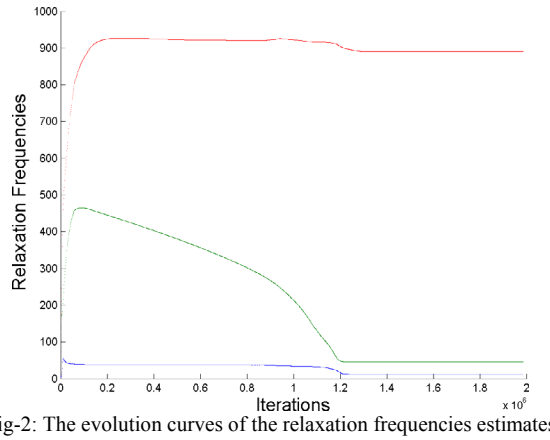

Fig-2: The evolution curves of the relaxation frequencies estimates

The number of assumed relaxation modes is increased to five. The initial guess is shown in table-4 below:

ζs (0)	0	50.1	90.5	120	200	300
Cs (0)	0.7	3.8	4.2	2.8	3	5

Table-4: Initial guess of the relaxation frequencies

The final estimates are shown in table-5 and the evolution of the relaxation frequencies is shown in figure-3. As can be seen, three assumed components merged into one value close to a base truth components. The sum of the strengths of these components is close to the base truth strength. The remaining components converged to values and strengths close to the base truth components.

ζf	0	8.7	8.7	8.7	45.7	890
Cf	0.494	0.293	0.293	0.293	1.121	2.995

Table-5: Final estimates of the relaxation frequencies and their magnitudes

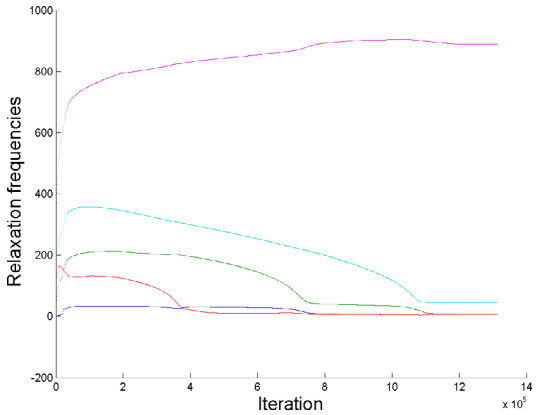

Fig-3: The evolution curves of the relaxation frequencies estimates

2. Robustness in the presence of noise

Here the effect of noise on the estimation method is examined. The base truth relaxation modes in table-1 are used in the test. The complex spectrum is sampled at 50 points that are uniformly distributed on the interval [2π, 600π]. Seven relaxation frequencies are assumed. The values of these frequencies and their magnitudes are shown in table-6.

ζs (0)	0	30	40	200	300	500	700	800
Cs (0)	0.7	3.8	4.2	2.8	3	5	4	4

Table-6: Initial guess

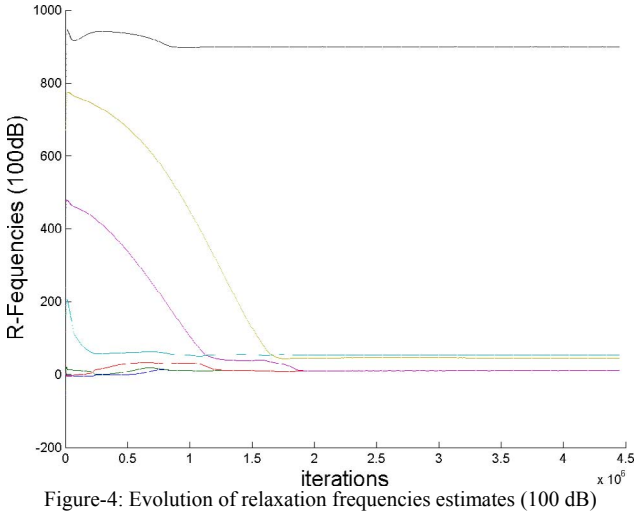

Figure-4: Evolution of relaxation frequencies estimates (100 dB)

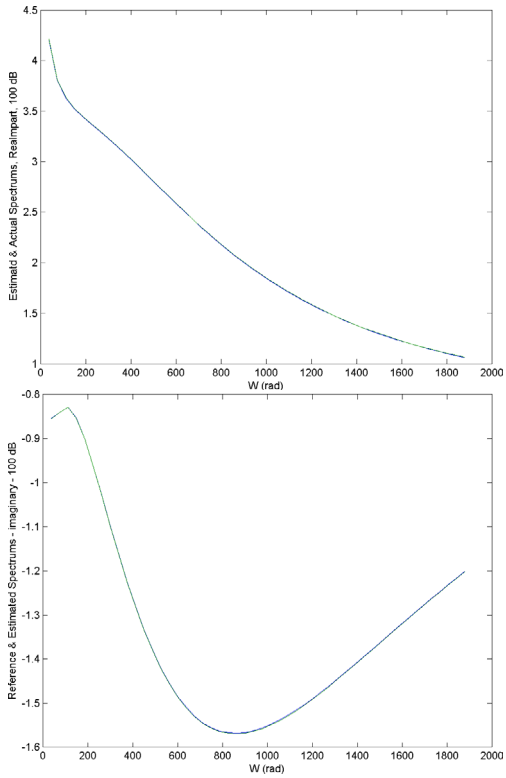

Figure-5: Real and imaginary parts of the base-truth (blue) and estimated (green) spectrums (100 dB)

The process is evaluated for three noise levels: low (SNR 100 dB), medium (SNR 40 dB) and high (SNR 20 dB). The estimated parameters are shown in table-7.

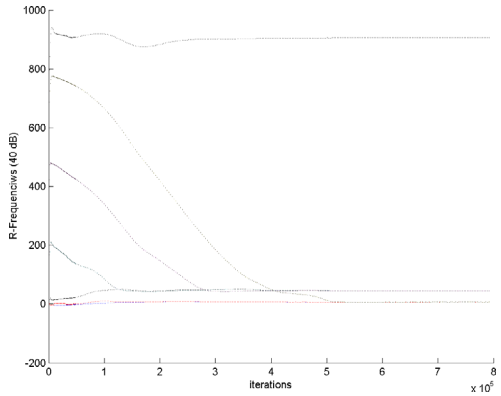

Figure-6: Evolution of relaxation frequencies estimates (40 dB)

SNR=100 dB		SNR=40 dB		SNR=20 dB	
ζf_i	cf_i	ζf_i	cf_i	ζf_i	cf_i
0	0.5027	0	0.4627	0	0.8023
11.4855	0.2219	8.2618	0.2645	15.5779	0.9803
11.4855	0.2219	44.579	0.3944	15.5779	0.9803
11.4855	0.2219	8.2618	0.2645	15.5779	0.9803
53.6164	0.5612	44.579	0.3944	86.1780	0.3929
11.4855	0.2219	44.577	0.3930	46.4476	-0.602
44.7444	0.4419	8.2633	0.2638	86.1780	0.3929
899.987	3.0024	904.56	2.9823	867.118	3.0245

Table-7: Final estimates

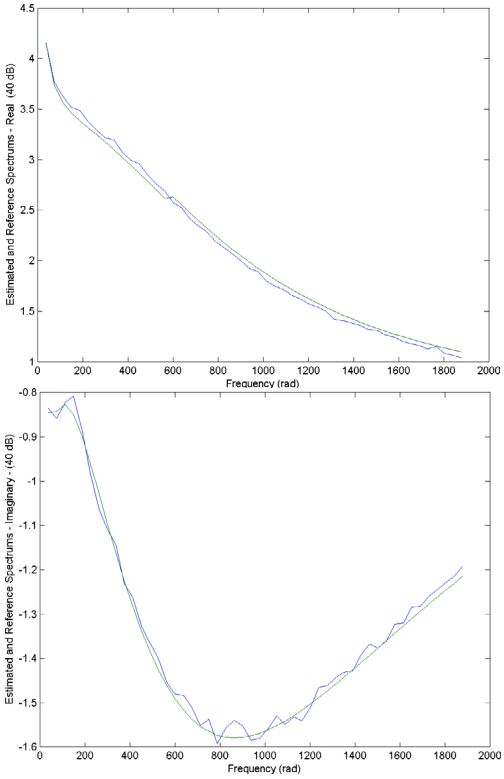

Figure-7: Real and imaginary parts of the base-truth (blue) and estimated (green) spectrums (40 dB)

The evolution of the relaxation frequencies for SNR= 100 dB is shown in figure-4. The superfluous components merged to values very close to the base-truth components. The base-truth and estimated spectrums (both real and imaginary parts) are shown in figure-5. As can be seen the estimated relaxation spectrum is almost identical to the base truth one.

Decreasing SNR 40 dB did not affect much the behavior of the procedure. The same observation for the SNR 100 dB case still hold. Actually, the addition of some nose seems to improve the quality of the estimates. The evolution of the relaxation frequency is shown in figure-6. The base-truth and estimated spectrums are shown in figure-7.

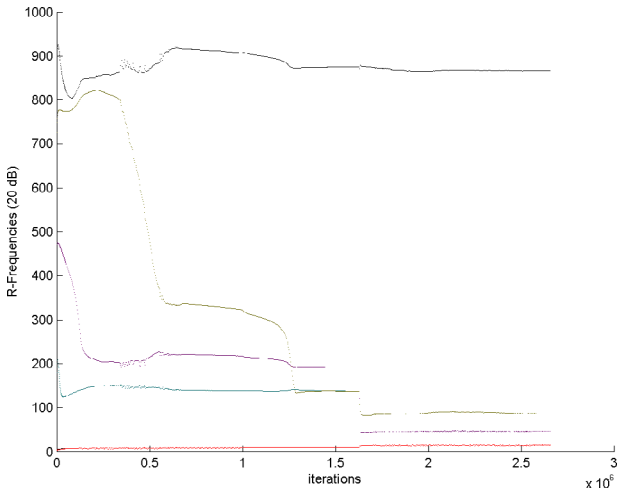

Figure-8: Evolution of relaxation frequencies estimates (20 dB)

The performance of the method remains acceptable even when SNR drops to as low as 20 dB. The evolution curves of the frequencies are in figure-8 and the spectrum estimates in figure-9.

3- Relaxation mode hypothesis testing

A scenario may be encountered where one is interested in detecting specific relaxation frequencies that correspond to certain buried objects of interest. In this case, the values of the relaxation frequencies of interest are fixed. Only their magnitudes are estimated to indicate their presence. This situation is tested below where a reflected base-truth signal with relaxation frequencies shown in table1 is used. The complex spectrum is evaluated at the same 17 frequencies given in example-1.

A set of seven fixed relaxation frequencies containing the correct ones are assumed (table-8). Only the magnitudes are allowed to vary. The final estimates are shown in table-9. As can be seen the magnitudes of the false frequencies dropped close to zero. The magnitudes of the correct ones converged close to the base-truth values. The evolution curves of the magnitudes are shown in figure-10.

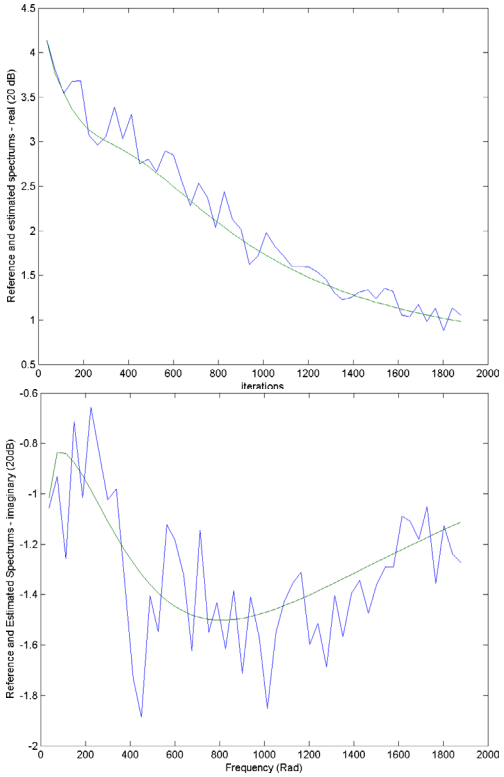

Figure-9: Real and imaginary parts of the given and estimated spectrums (20 dB)

ζ	0	10	50	100	400	500	700	900
C	0.7	3.8	4.2	2.8	3	5	4	4

Table-8: Assumed fixed relaxation frequencies and their magnitudes

ζs	Cf
0	0.4998
10	1.0004
50	0.9992
100	.0011
400	-0.0171
500	0.0320
700	-0.0252
900	3.009

Table-9- 13: Final estimates

V. CONCLUSIONS

A robust technique for blindly and jointly identifying the order of a GPR discrete relaxation spectrum and estimating its parameters is suggested. Early investigation shows that the method is robust, efficient and hardware-friendly.

We are currently focusing our activities to develop the method along two directions. The first direction is to experimentally verify the performance of the method. The other has to do with theoretically investigating the behavior of the method in terms of its ability to converge to the true estimates along with its behavior in the presence of noise.

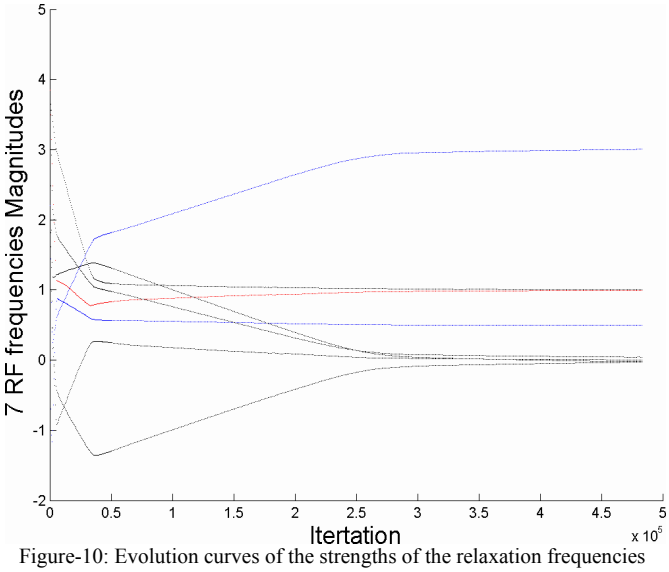

Figure-10: Evolution curves of the strengths of the relaxation frequencies assumed in table-8.

ACKNOWLEDGMENT

The authors gratefully acknowledge the assistance of king Fahad University of Petroleum and Minerals.

REFERENCES

[1] Harry M. Jol , Ed., "Ground Penetrating Radar Theory and Applications", Elsevier, 2009 ISBN: 978-0-444-53348-7

[2] David. J. Daniels Ed., "Ground penetrating radar", 2nd Edition, the institution of electrical engineers, 2004

[3] Yu. Feldman, Yu. A. Gusey, M. A. Vasilyeva, "Dielectric Relaxation Phenomena in Complex Systems: Tutorial", The Kazan Federal University Institute of Physics, 2012, p.134

[4] Marshall D.J. and Madden T.R. 1959. Induced polarization, a study of its causes. Geophysics 24, 790–816.

[5] Vladimir Burtman, Michael S. Zhdanov, "Induced polarization effect in reservoir rocks and its modeling based on generalized effective-medium theory", Resource-Efficient Technologies 1 (2015) 34–48

[6] Kenneth S. Cole and Robert H. Cole, J. Chem. Phys. 9, 341 (1941); http://dx.doi.org/10.1063/1.1750906

[7] Hugues Garnier, "Direct continuous-time approaches to system identification. Overview and benefits for practical applications", European Journal of Control Volume 24, July 2015, Pages 50–62

[8] Robinson, E.A., "A historical perspective of spectrum estimation", Proceedings of the IEEE, 1982, Page(s):885- 907

[9] S. M. KAY, S. MARPLE, JR., "Spectrum Analysis-A Modern Perspective", Proceedings of the IEEE, VOL. 69, NO. 11, NOVEMBER 1981, pp.1380-1419

[10] Huang, JH; Baird, DG, "Ratio of dynamic moduli and estimation of relaxation times," J. Rheol. 46, pp. 777-795 (2002); http://dx.doi.org/10.1122/1.1485278

[11] Erik Appel Jensen, "Determination of discrete relaxation spectra using Simulated Annealing", J. Non-Newtonian Fluid Mech. 107 (2002) 1–11

[12] Mead, D. W., ''Numerical interconversion of linear viscoelastic material functions,'' J. Rheol. 38, 1769–1795, 1994.

[13] Honerkamp, J. and J. Weese, ''Determination of the relaxation spectrum by a regularization method,'' Macromolecules 22, 4372–4377, 1989.

[14] Winter, H. H., ''Analysis of dynamic mechanical data: Inversion into a relaxation time spectrum and consistency check,'' J. Non-Newtonian Fluid Mech. 68, 225–239, 1997.

[15] Mustapha, S. M. F. D. S. and T. N. Phillips, ''A dynamic nonlinear regression method for the determination of the discrete relaxation spectrum,'' J. Phys. D 33, 1219–1229, 2000.

[16] Mu-Hsin Wei, Waymond R. Scott, Jr., James H. McClellan, "Robust Estimation of the Discrete Spectrum of Relaxations for Electromagnetic Induction Responses", IEEE Transactions on Geosciences and Remote Sensing, Vol. 48, No. 3, March 2010, pp.1169-1179

[17] Ali Cafer Gurbuz, James H. McClellan, Waymond R. Scott Jr., "Compressive sensing of underground structures using GPR", Digital Signal Processing 22 (2012) 66–73

[18] Mu-Hsin Wei, Waymond R. Scott, Jr., James H. McClellan, "Adaptive Prefiltering for Nonnegative Discrete Spectrum of Relaxations", IEEE Geosciences and Remote sensing Letters, Vol. 12, No. 5, May 2015, pp. 1018-1022

[19] N. Florsch, C. Camerlynck and A. Revil, "Direct estimation of the distribution of relaxation times from induced-polarization spectra using a Fourier transform analysis", Near Surface Geophysics, 2012, 10, 517-531 doi:10.3997/1873-0604.2012004

[20] Ting Hei Wana, Mattia Saccoccioa, Chi Chena, Francesco Ciuccia, "Influence of the Discretization Methods on the Distribution of Relaxation Times Deconvolution: Implementing Radial Basis Functions with DRTtools", Electrochimica Acta 184 (2015) 483–499

[21] M. Baumgaertel, H. Winters, "Interrelation between continuous and discrete relaxation time spectra", Journal of Non-Newtonian Fluid Mechanics, Vol. 44, 1992, pp.15-36